Spin dynamics in the singlet-singlet ground state magnet $LiTb_xY_{1-x}F_4$; a neutron scattering study

1990 J. Phys.: Condens. Matter 2 2383

(http://iopscience.iop.org/0953-8984/2/10/006)

J. Phys.: Condens. Matter **2** (1990) 2383–2396. Printed in the UK

Spin dynamics in the singlet–singlet ground state magnet $LiTb_xY_{1-x}F_4$; a neutron scattering study

R G Lloyd† and P W Mitchell‡

† Institut Laue–Langevin, BP156X, 38042 Grenoble Cédex, France

‡ Department of Physics, University of Manchester, Manchester M13 9PL, UK

Received 11 October 1989

Abstract. A neutron inelastic scattering study is presented of the spin dynamics at and above T_C in the singlet–singlet ground state ferromagnet $LiTb_xY_{1-x}F_4$ for $x = 1.0$ and $x = 0.6$. Above T_C the dynamics are found to be very well described by an overdamped relaxation-coupled oscillator (RCO) lineshape with the frequencies of magnetic excitons given by the mean-field dispersion relation. The damping parameter is found to be much greater in the pure material than in the dilute material. At T_C the RCO lineshape is found not to fit the data for small $\boldsymbol{q}$, rather a Lorentzian function has been used to extract a characteristic frequency. In the pure system the value for the dynamical critical exponent z is found to be 0.79 ± 0.26. In the dilute system an extra component to the scattering is found to obscure the asymptotic critical behaviour for small $\boldsymbol{q}$. However for larger $\boldsymbol{q}$ a power-law dependence of the characteristic frequency is found with exponent 0.8 ± 0.1.

1. Introduction

$LiTb_xY_{1-x}F_4$ has been shown to be an excellent example of a singlet–singlet ground state magnet (Youngblood *et al* 1982), in which the two lowest-lying single-ion states of the rare earth ion are non-magnetic singlets and the magnetic moments are induced in the crystal by the interactions between the rare-earth ions. The Hamiltonian of such a system is isomorphic to that of an Ising model in a transverse magnetic field,

$$H = -\sum_{ij} J_{ij}\boldsymbol{\sigma}_i^z\boldsymbol{\sigma}_j^z - \Delta\sum_i \boldsymbol{\sigma}_i^x \tag{1}$$

where Δ is the energy separation of the crystal-field-split ground state of the terbium ions. This simple, quantum Hamiltonian may be used to model a number of diverse problems in the theory of phase transitions (for a detailed list see Stinchcombe 1973). For example it also describes the ferroelectric transition in KH_2PO_4 where the energy Δ is the quantum mechanical tunnelling energy of the protons in their double-well potentials.

As regards the static critical phenomena, the second term in the Hamiltonian becomes technically irrelevant apart from modifying the transition temperature (Young 1975 and references therein) and pure $LiTbF_4$ has been used in the past as a model dipolar-coupled Ising system (Als-Nielsen *et al* 1974, 1975, Ahlers *et al* 1975, Holmes *et al* 1975, Als-Nielsen 1976). This system is something of a test-bed for the renomalisation group theories of critical phenomena. For the dipolar-coupled Ising ferromagnet the

0953-8984/90/102383 + 14 $03.50

marginal dimension is three and therefore the renormalisation group theory predicts that mean-field theory applies with small, exactly calculable logarithmic corrections. This has been well established both theoretically and experimentally and the behaviour at marginal dimensionality is one of the best understood parts of the theory of critical phenomena.

The disordered $LiTb_xY_{1-x}F_4$ system has also been studied, partly because of the theoretical work of Aharony (1976) which predicted different static critical behaviour in the pure and random systems. There was also a possibility of the existence of a spin-glass phase in the dilute limit (Stephen and Aharony 1981). More recently, a neutron critical scattering study of $LiTb_{0.3}Y_{0.7}F_4$ (Kjaer *et al* 1989) showed the existence of an anomalous component of the scattering at small wavevector transfers.

Despite significant experimental and theoretical effort (for a review of the theoretical work see Dumont 1984) the nature of the spin dynamics of the transverse Ising model has still not been fully established. In the regime where the transverse field is comparable in magnitude to the interaction between the spins ($\Delta \simeq \langle J_{ij}^2 \rangle^{1/2}$) the system displays collective excitations both above and below T_C. These excitations soften as T approaches T_C. This is in analogy with the 'soft-mode' models used to describe structural phase transitions.

Much of the controversy which has surrounded the spin dynamics in the transverse Ising model has concerned the lineshape of these excitations. The central issue is whether or not the response function displays a quasi-elastic central peak as well as peaks at the finite exciton frequencies, and if so, whether this central peak is an intrinsic feature of the model Hamiltonian or whether its existence is due to a coupling to some other degree of freedom. Neither is it clear to what extent the dynamics in the critical region are governed by the softening excitonic modes or whether they are dominated by other relaxation mechanisms which may perhaps be better described within a kinetic Ising model framework.

Away from the critical region the excitation frequencies are given, within a mean-field approach (De Gennes 1963, Wang and Cooper 1968), by the dispersion relations

$$\omega_0(\boldsymbol{q}) = \Delta(1 - \tanh(\Delta/2kT)J(\boldsymbol{q})/2\Delta)^{1/2} \tag{2}$$

for $T > T_C$, and by

$$\omega_0(\boldsymbol{q}) = \Delta(J(0)^2/4\Delta^2 - J(\boldsymbol{q})/J(0))^{1/2} \tag{3}$$

for $T < T_C$. The mean-field theory also gives the value of the transition temperature T_C as a function of Δ and $J(0)$, from the relation

$$\coth(\Delta/2kT_C) = J(0)/2\Delta. \tag{4}$$

For a dilute magnet $J(0)$ scales linearly with the proportion of the magnetic species which gives rise to a linear boundary between the ferromagnetic and paramagnetic phases in the phase diagram for $LiTb_xY_{1-x}F_4$.

Previous neutron scattering measurements (Youngblood *et al* 1982) of the dynamics in this material showed a qualitative difference between the form of the spectral response with $x = 0.97$ and $x = 0.38$. For $x = 0.97$ they show a resolution-limited central peak, with no evidence for the existence of excitonic modes. For $x = 0.38$ a central peak is observed which coexists with finite frequency excitonic sidebands.

The controversy over the lineshape was to some extent cleared up, at least for the pure system, by the experimental work of Kötzler *et al* (1988) who showed that a

relaxation-coupled oscillator lineshape (a form which was also first used in the structural phase transition context (Shirane and Axe 1971) gave the best fit to their measurements of the ratio of the real to the imaginary part of the bulk AC susceptibility. This form for the lineshape arises because of a coupling between the oscillating exciton modes and the exponentially relaxing σ^x component of the spins, although the precise nature of this coupling is not clear. This study gave no information about the q-dependence of the energy spectrum.

We present, in this paper, a high resolution neutron inelastic scattering study of the spin dynamics in $LiTb_xY_{1-x}F_4$ for $x = 1$ and $x = 0.6$. We examine the form of the spectral response above T_C along with its wavevector and temperature dependence. We also measure the critical dynamics at T_C. We present measurements of the dynamical critical exponent z and examine the evolution of the lineshape as $q \rightarrow 0$ at T_C.

2. $LiTb_xY_{1-x}F_4$

$LiTb_xY_{1-x}F_4$ has an average scheelite crystal structure, with space group $I4_1/a$. For $x = 1$ there are four Tb^{3+} ions in each body-centred tetragonal unit cell. The Y^{3+} ions act as a random non-magnetic diluent with a closed $4p^6$ electron configuration. The electron configuration of the Tb^{3+} ion is $4f^8$ which has a $^7F_6$ ground term, and the degeneracy of the states is lifted by the crystal electric field. The ground state was once thought to be a degenerate ($m_j = \pm 6$) doublet, but in fact the lowest lying states are a pair of non-magnetic Γ_2 singlets separated in energy by 1.40 ± 0.14 K (Laursen and Holmes 1974, Margarino *et al* 1980). This splitting arises because the crystal field mixes a small fraction of the $m_j = \pm 2$ states with the $m_j = \pm 6$ states. The next nearest excited states lie at least 170 K higher in energy and so play no role in the low temperature behaviour.

The interactions between the Tb^{3+} ions have been shown to be predominantly dipolar in nature (Holmes *et al* 1975) with the exchange contributing about 10% of the total interaction energy.

The samples we used were high-quality single crystals of pure $LiTbF_4$ and $LiTb_{0.6}Y_{0.4}F_4$ grown by R C C Ward and M Cherrill at the Oxford Clarendon Laboratory crystal growing facility. They were in the form of cylinders of length approximately 20 mm and diameter 7 mm with the $[1, \bar{1}, 0]$ direction along the axis of the cylinder. ^7Li isotope was used in the crystals since ^6Li, which has approximately 7.5% natural abundance, is strongly neutron-absorbing. Both crystals were optically clear and colourless.

3. Experimental details

The experiments were performed using the triple axis spectrometer IN12 at the Institut Laue–Langevin, with pyrolytic graphite for both the monochromator and the analyser. In all cases a beryllium filter was used on the beam incident on the sample to remove the order contamination. The samples were mounted in variable temperature helium cryostats, which were pumped to obtain the low temperatures required. The scans were made with various fixed incident wavevectors and collimator combinations giving the resolution conditions required. The collimator values in minutes for monochromator–sample, sample–analyser and analyser–detector respectively were for the pure system; 30/30/30 with incident neutron wavevector $k_I = 1.05$ Å^{-1} giving the caliper energy

resolution width (as measured with a vanadium sample) to be 5.8 GHz (FWHM), 30/30/30 with $k_I = 1.01$ Å^{-1} giving 4.6 GHz, 10/10/10 with $k_I = 1.01$ Å^{-1} giving 2.6 GHz, and for the dilute system 20/20/20 with $k_I = 1.0$ Å^{-1} giving 2.6 GHz, 10/10/10 with $k_I = 1.0$ Å^{-1} giving 2.3 GHz, and 30/30/30 with $k_I = 1.1$ Å^{-1} giving 7.4 GHz.

In all cases a check was made on the energy resolution by measuring the scattering from a vanadium sample which is a predominantly elastic incoherent scatterer.

The crystal of pure $LiTbF_4$ was mounted with the $[1,\bar{1},0]$ direction vertical and the $LiTb_{0.6}Y_{0.4}F_4$ with the $[0,0,1]$ direction vertical.

The transition temperatures of the crystals were measured by monitoring the temperature dependence of the magnetic Bragg scattering at $(1,1,2)$ in the pure crystal and $(2,0,0)$ in the dilute crystal and the critical scattering at $(0.98,0.98,2)$ and $(1.98,0,0)$ respectively. T_C for the pure $LiTbF_4$ was measured to be 2.89 ± 0.01 K and for $LiTb_{0.6}Y_{0.4}F_4$, 1.54 ± 0.01 K.

The energy spectra were measured by performing scans at fixed wavevector transfers $(\zeta,\zeta,0)$ in the pure system and $(\zeta,0,0)$ in the dilute system.

4. Models and data analysis

For these measurements the instrumental resolution corrections to the data were of paramount importance for two reasons. First the scans were made at relatively small scattering angles and so the resolution function was highly anisotropic. This anisotropy may very easily have produced distortion in the observed energy spectra since the scattering functions that we were measuring are also very anisotropic in $\boldsymbol{q}$ due to the dipolar interactions. Secondly the low energy scale of the spin fluctuations in these systems means that parts of the experiments were performed at the limit of the highest resolution currently obtainable on a three-axis spectrometer. The energy widths of the spectra were in most cases barely larger than the energy resolution.

For a neutron triple-axis spectrometer the counting rate at the detector may be written as

$$J(\boldsymbol{q}_0,\omega_0) = \int_{\text{all } \boldsymbol{q}} \int_{-\infty}^{\infty} \mathrm{d}^3\boldsymbol{q}\,\mathrm{d}\omega\; S(\boldsymbol{q},\omega)R(\boldsymbol{q}-\boldsymbol{q}_0,\omega-\omega_0) \tag{5}$$

the resolution function being approximated as the Gaussian form

$$R(\boldsymbol{q}-\boldsymbol{q}_0,\omega-\omega_0) = R_0 \exp(-\tfrac{1}{2}\boldsymbol{x}^{\mathrm{T}}\mathbf{M}\boldsymbol{x}) \tag{6}$$

where $\mathrm{x} = (\boldsymbol{q}-\boldsymbol{q}_0,\omega-\omega_0)$, and $\mathbf{M} = \mathbf{M}(\boldsymbol{q}_0,\omega_0)$ is a symmetric matrix whose elements are functions of the instrumental parameters. The constant R_0 is given by

$$R_0 = A(V_I V_F/4\pi^2)\sqrt{\det \mathbf{M}} \tag{7}$$

where the constant A contains generic factors such as the detector and monitor efficiencies, the reflectivity of the analyser, and the attenuation due to neutron absorption by anything that may be in the neutron path (such as the beryllium filter, the collimators etc).

V_I and V_F are the resolution volumes in phase space for the primary and secondary spectrometers respectively. The effect of V_I was removed by counting the points in the

scans for a fixed count in a monitor placed after the monochromator and before the sample. V_F is approximately given by,

$$V_F = k_F^3 \cot \theta_A \tag{8}$$

where θ_A is the Bragg angle at the analyser and k_F is the scattered neutron wavevector. The four-dimensional integral in equation (5) was performed numerically for model scattering functions $S(\boldsymbol{q}, \omega)$ and the model parameters refined using a fitting algorithm to minimise a merit function χ^2, defined assuming the neutron counts to be distributed according to Poisson statistics.

The data taken above T_C and the data taken at T_C were analysed using different models so we shall examine each case in turn in the sections which follow.

5. Measurements above T_C

5.1. The relaxation-coupled oscillator

The data taken above T_C in the two crystals were analysed using the relaxation-coupled oscillator (RCO) model given by Kötzler *et al* (1988) for $LiTbF_4$. This model has also been extensively used to model structural phase transitions within a soft-mode approach. The difference in this case is that we find a highly *overdamped* RCO to be necessary to fit the data and so the energy profile does not easily separate into the sum of a centrally peaked Lorentzian and a damped harmonic oscillator.

In this model the magnetic susceptibility is given by,

$$\chi(\boldsymbol{q}, \omega) = (\chi_0 \Delta^2 / T)(\omega_0(\boldsymbol{q}, T)^2 - \omega^2 + i\omega\gamma(\omega))^{-1} \tag{9}$$

where

$$\gamma(\omega) = \delta^2/(\varphi + i\omega) + \gamma_0. \tag{10}$$

All the $\boldsymbol{q}$ and temperature dependence (apart from the $1/T$ Curie law) is contained in $\omega_0(\boldsymbol{q}, T)$ which softens as the ordering transition is approached (i.e. $\boldsymbol{q} \rightarrow \boldsymbol{0}$ and $T \rightarrow T_C$). There are three other parameters which are assumed to be independent of wavevector and temperature. δ is a coupling constant between the oscillating mode and the relaxing mode, φ gives a characteristic frequency for the relaxing mode and γ_0 is the damping constant of the oscillating mode. The singlet–singlet splitting energy Δ is included for dimensional consistency.

The quantity measured in a neutron inelastic scattering experiment is proportional to the imaginary part of this susceptibility which is given in this case by the lineshape function,

$$\chi''(\boldsymbol{q}, \omega) = \frac{-\chi_0 \omega \Delta^2}{T} \left(\frac{\delta^2}{(\varphi^2 + \omega^2)} \varphi + \gamma_0 \right) \left\{ \left[\omega_0^2 - \omega^2 \left(1 + \frac{\delta^2}{(\varphi^2 + \omega^2)} \right) \right]^2 + \left(\omega\varphi \frac{\delta^2}{(\varphi^2 + \omega^2)} + \omega\gamma_0 \right)^2 \right\}^{-1}. \tag{11}$$

In the limit $\gamma_0 \ll \delta^2/\varphi$ and $\omega_0^2 + \delta^2 \gg \varphi$ this expression may be separated into the sum of a Lorentzian centred at $\omega = 0$ and a damped harmonic oscillator of pole frequency

$\omega_0^2 + \delta^2$. The centrally peaked Lorentzian has width $\Gamma_{Lor} = \varphi\,\omega_0^2/(\omega_0^2 + \delta^2)$ and amplitude,

$$A_{Lor} = \delta^2/\omega_0^2(\omega_0^2 + \delta^2). \tag{12}$$

We found that this limit was not satisfied in our data since $\gamma_0 > \delta^2/\varphi$. However we expect some features of this decomposition to remain. For example, within the model the width of the central peak goes to zero as ω_0^2 and its intensity goes as ω_0^{-2}. So as the transition is approached there is a critical slowing down and a divergence in the intensity of the central peak. The dynamical exponent given in this model is therefore equal to 2 since $\omega_0^2 \propto |\boldsymbol{q}|^2$. The details of the model are of crucial importance here because if there were no coupling to the relaxing mode the characteristic frequency would be simply ω_0 and therefore the dynamic exponent would be equal to 1.

5.2. Results

We found the lineshape equation (11) to give a much better description of the data above T_C than a simple Lorentzian and so we fitted it to all of the data above T_C in both pure $LiTbF_4$ and $LiTb_{0.6}Y_{0.4}F_4$. For each crystal all the data were fitted simultaneously using the values for the exciton frequencies $\omega_0(\boldsymbol{q}, T)$ given by mean-field theory, equation (2). Before this simultaneous fit was carried out each scan was fitted individually to the RCO lineshape and a value for $\omega_0(\boldsymbol{q}, T)$ found. No evidence was found in the data for any $\boldsymbol{q}$- or T-dependence in either γ_0, δ or φ.

In the dilute system data were taken at $\boldsymbol{q}$-values $(\zeta, 0, 0)$ RLU for $\xi = 0.1$ to 1.0 with energy range -120 GHz to 90 GHz at temperatures 1.8 K, 2.49 K and 3.96 K. These data were taken with a caliper energy resolution width of 7.4 GHz. The data with ξ between 0.1 and 0.6 were fitted simultaneously to the RCO model. The data taken at higher $\boldsymbol{q}$, out to the zone boundary, were also found to fit well to the RCO lineshape but with an exciton frequency slightly lower than that predicted by the mean-field dispersion relation (equation (2)). Some deviation in this sense is expected because of the symmetry requirement of zero gradient at the zone boundary.

We were able to fit to the low-$\boldsymbol{q}$ data using six variable parameters. Sample scans and the corresponding model calculations from this simultaneous fit are shown in figure 1 for constant wavevector transfer and in figure 2 for constant temperature. The exciton frequencies are marked by the vertical arrows. At this point there is no visible peak in the data although clear shoulders can be seen in some scans. The excitons are manifested by wide wings on a large central peak. The values of the parameters given by this fit are as follows, $\Delta = 30.03 \pm 0.04$ GHz, $\delta = 18.0 \pm 0.3$ GHz, $\varphi = 5.0 \pm 0.3$ GHz and $\gamma_0 = 57 \pm 2$ GHz. The Fourier transform of the interaction between the spins was found to be given by $J(\boldsymbol{q}) = A_1 - A_2|\boldsymbol{q}|^2$ with $A_1 = 0.068 \pm 0.001$ K and $A_2 = 0.12 \pm 0.01$ K Å^2. There should be another term in this interaction due to the anisotropy of the dipolar interaction, but its value could not be measured from the data and so was kept fixed at zero. It has a negligible effect on all the other parameters in the fit. The final value of the merit function χ^2 in the fit was 931 which is equivalent to 1.76 per degree of freedom.

For the pure $LiTbF_4$ our data were taken with slightly higher energy resolution (5.8 GHz caliper width) but each scan does not cover such a wide frequency range (-15 GHz to 10 GHz). This meant that often the exciton frequency lay outside our frequency range and we were unable to allow all the parameters in our model to vary in the fit. The value of the singlet–singlet splitting Δ was therefore kept fixed at the value obtained from the dilute system and all the other parameters allowed to vary. Data were

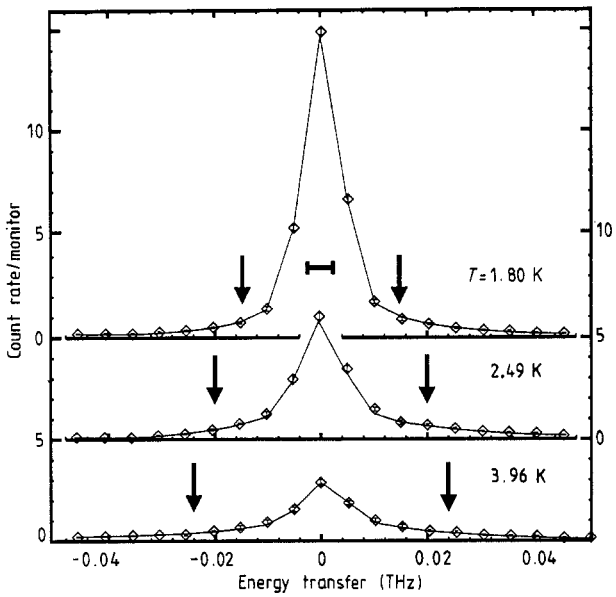

Figure 1. Scans taken at various temperatures above T_C at $\boldsymbol{q} = (0.2, 0, 0)$ RLU in $LiTb_{0.6}Y_{0.4}F_4$. The diamonds are the measured data points. The full line joins the points of the fitted function, as described in the text, calculated at the same frequency values. The arrows mark the magnetic exciton frequencies.

taken for $\boldsymbol{q} = (\zeta, \zeta, 0)$ RLU in the range $\zeta = 0.05$ to 0.4 at temperatures 3.14 K, 3.7 K, 4.3 K and 5.7 K. All the data were used in the simultaneous fit.

Sample scans and the corresponding model calculations are shown in figures 3 and 4 for constant wavevector transfer and constant temperature respectively. The exciton frequencies are marked by the vertical arrows as before.

To the individual scans we were also able to fit a Lorentzian shape function and indeed this was how we initially analysed the data (see Lloyd *et al* (1988) for a preliminary account). However, to do this we had to allow a varying background which was much larger than the measured background and therefore physically unrealistic. The RCO lineshape with the measured background clearly gives a better fit than the Lorentzian with floating background to all of the data above T_C.

The values of the parameters given by the fit are, $\delta = 21 \pm 1$ GHz, $\varphi = 7.1 \pm 0.6$ GHz and $\gamma_0 = 88 \pm 4$ GHz. The Fourier transform of the interaction between the spins was found to be given by $J(\boldsymbol{q}) = A_1 - A_2|\boldsymbol{q}|^2 - A_3(q_z/|\boldsymbol{q}|)^2$ where $A_1 = 0.115 \pm 0.001$ K and $A_2 = 0.23 \pm 0.01$ K Å^2 and the anisotropy parameter A_3 was kept fixed at the value given by Als-Nielsen *et al* (1974) of 0.173 K. Again this was found to have a negligible influence on the fit. In this case, the final value of the merit function χ^2 was 543 which is equivalent to 1.37 per degree of freedom.

Perhaps the most noticeable feature of these results is that the damping parameter γ_0 is so much larger in the pure $LiTbF_4$. This explains the qualitative difference in the form of the power spectra measured in the pure and dilute systems by Youngblood *et al* (1982) who only observed the excitons in the *dilute* system. We show here that the frequency spectrum above T_C in both the pure and the dilute systems may be described by the same functional form but with a much stronger damping in the pure system. The

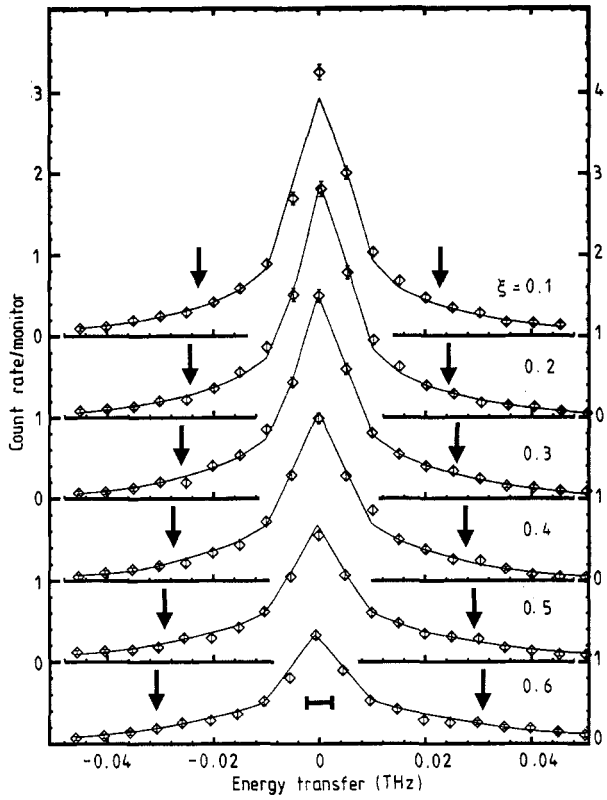

Figure 2. Scans taken at various wavevector transfers at $T = 3.96$ K (for $\boldsymbol{q} = (\xi, 0, 0)$ RLU) in $LiTb_{0.6}Y_{0.4}F_4$. The diamonds mark the measured data points and the full lines join the points of the calculated model function fitted as described in the text. The arrows mark the magnetic exciton frequencies.

exciton frequencies are found to be well described by the mean-field theory. Our results for the other parameters are all in excellent agreement with the AC susceptibility measurements of Kötzler *et al* (1988) and with the ESR values for Δ of Laursen *et al* (1974) and Margarino *et al* (1980) of 30 ± 10 GHz for $LiTbF_4$.

6. Critical dynamics at T_C

6.1. The model

At T_C the RCO model that successfully describes the data above T_C was found to break down. At small $\boldsymbol{q}$ the lineshape could no longer be fitted by the form given in equation (11) even with very small values for ω_0. The data were better fitted with a Lorentzian lineshape although at the smallest $\boldsymbol{q}$-values even this was found to be too high in the wings. In these cases, however, the Lorentzian width was less than 25% of the energy resolution width and so reliable parameters could not be extracted from the data in any case. The power spectrum is known to fall off faster than a Lorentzian for sufficiently high frequencies corresponding to the highest frequencies available in the system. For larger wavevector transfers the RCO lineshape was found to be regained as can be seen

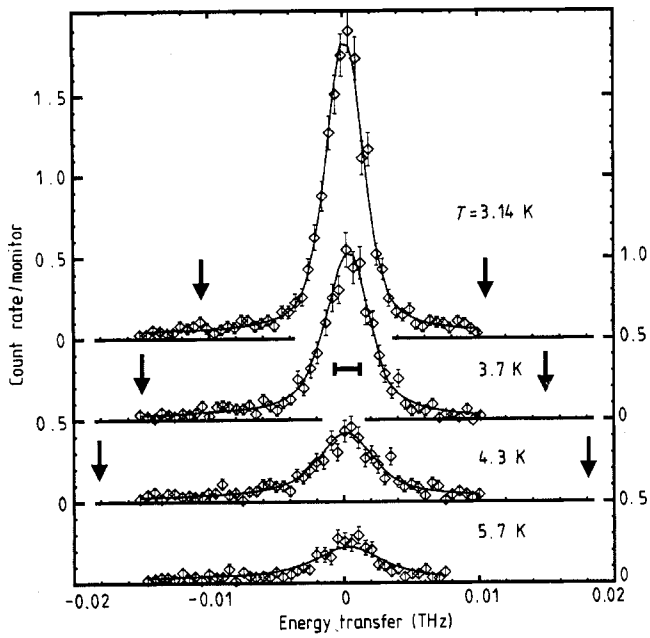

Figure 3. Scans taken at various temperatures above T_C at $\boldsymbol{q} = (0.02, 0.02, 0)$ RLU in pure $LiTbF_4$. The diamonds are the measured data points (with their errors). The full curves join the points of the calculated function fitted to the data as described in the text. The arrows mark the magnetic exciton frequencies.

from a comparison of the two lineshapes in figure 5. However most of the spectral weight lies in the central peak (figure 5 shows the logarithm of the intensity) and therefore in order to extract consistently a characteristic frequency and to measure the dynamical critical exponent a Lorentzian spectral weight function with a fixed background was used for all the scans taken at T_C. The systematic error on the characteristic frequency inherent in this procedure was estimated as 0.5% for the scan taken at the highest $\boldsymbol{q}$ which is much smaller than the error given by the fitting procedure for the Lorentzian width (typically 2–5%).

The details of the model are as follows. To separate the frequency structure from the $\boldsymbol{q}$-structure in $S(\boldsymbol{q}, \omega)$ we make the usual factorisation into a static wavevector-dependent susceptibility and a normalised spectral weight function

$$S(\boldsymbol{q}, \omega) = (n(\omega) + 1)\chi_q F(\boldsymbol{q}, \omega) \tag{13}$$

where $n(\omega)$ is the Bose occupation factor and $F(\boldsymbol{q}, \omega)$ is normalised in the usual way,

$$\int_{-\infty}^{+\infty} \mathrm{d}\omega \, F(\boldsymbol{q}, \omega) = 1. \tag{14}$$

The form of χ_q for pure $LiTbF_4$ was measured by Als-Nielsen (1976) to be

$$\chi_q^{-1} = \kappa^2 + |\boldsymbol{q}|^2 + g(q_z/|\boldsymbol{q}|)^2 \tag{15}$$

where $g = 1.3 \pm 0.1$ Å^{-1}. We used this form with g fixed at 1.3 Å^{-1} since its value could not be extracted from our data. This form was also used for the dilute system with the

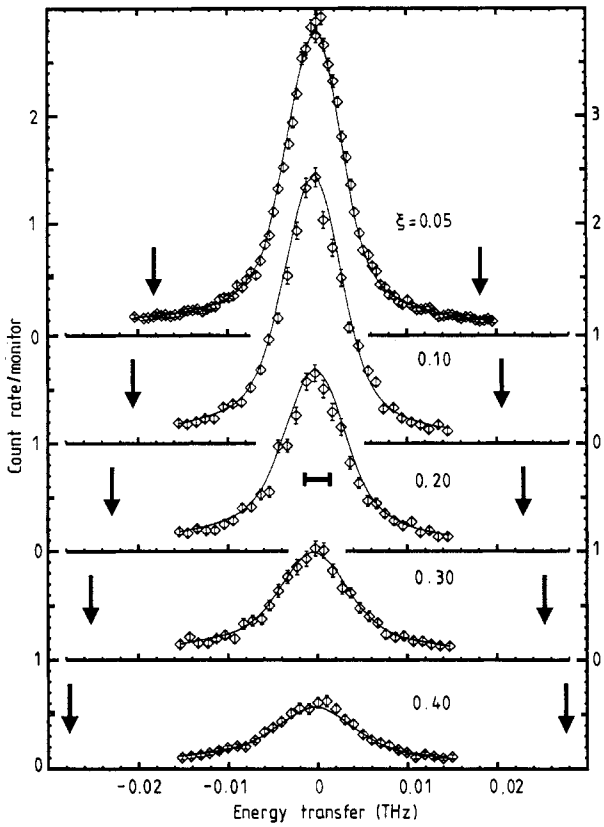

Figure 4. Scans taken at various wavevector transfers at $T = 4.33$ K (for $\boldsymbol{q} = (\zeta, \zeta, 0)$ RLU) in pure $LiTbF_4$. The diamonds mark the measured data points (with their errors) and the full curves join the points of the calculated model function as described in the text. The arrows mark the magnetic exciton frequencies.

same value of g. There is a possibility that in the dilute system the value of g may be larger than for the pure system since dilution may be expected to increase the effect of antiferromagnetic interactions between the spins (which occur in the basal plane) relative to the out-of-plane ferromagnetic interactions. However, our data did not give sufficient information for us to justify using a different value for g. It has to be changed a long way from 1.3 $Å^{-1}$ before having any effect on the parameters obtained from the fits.

The spectral weight function we used was thus the Lorentzian

$$F(\boldsymbol{q}, \omega) = (1/\pi)\,\Gamma(\boldsymbol{q})/(\Gamma(\boldsymbol{q})^2 + \omega^2) \tag{16}$$

with an anisotropic dynamical scaling form for the characteristic frequency,

$$\Gamma(\boldsymbol{q}) = \Gamma_0(|\boldsymbol{q}|^2 + g(q_z/|\boldsymbol{q}|)^2)^{z/2}\Omega(\kappa/|\boldsymbol{q}|). \tag{17}$$

This anisotropic form reflects the fact that the critical region is much narrower in the z-direction than the x- and y-directions. Therefore the energy width may be expected to increase much faster with q_z than with q_x or q_y. The approach to the critical point may nonetheless be described by a single correlation length which is super-diverging in the

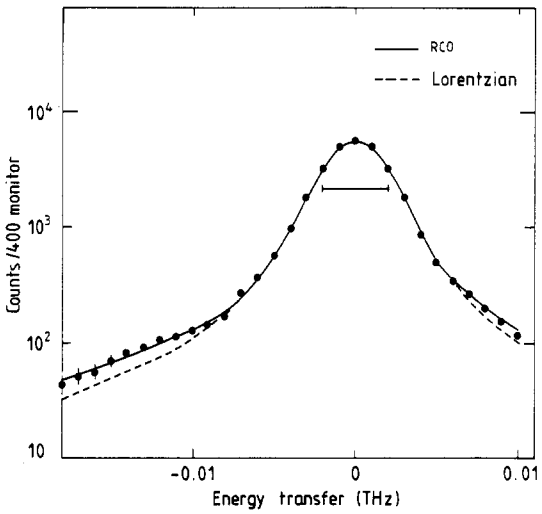

Figure 5. A comparison of the Lorentzian (broken curve) and the relaxation coupled oscillator (full curve) lineshapes for the energy spectrum measured at $\boldsymbol{q} = (0.1, 0.1, 0)$ RLU and $T = 2.89$ K ($= T_C$) in $LiTbF_4$. Note the logarithmic scale for the counts.

z-direction. This point is discussed in detail in the studies of the static critical phenomena (Als-Nielsen 1976).

No one combination of the parameters z, κ and Γ_0 could be found to describe all of the data in either the pure or the dilute systems. This meant that a single simultaneous fit to the data using a single model could not be obtained. Instead an alternative approach to making consistent resolution corrections was used. Initial fixed values were assumed for z and κ ($z = 2$ and $\kappa = 0.01$), Γ_0 and an overall scale being used as fitting parameters for each scan individually. Then $\Gamma(\boldsymbol{q})$ and $\chi(\boldsymbol{q})$ could be reconstructed for each scan and plotted against $\boldsymbol{q}$. From these plots better values for z and κ could be extracted. The scans were then refitted with these values. In principle this iterative process could have been repeated to refine further the values obtained although in neither case was this found to be necessary.

6.2. Results

6.2.1. $LiTbF_4$. A plot of the characteristic frequency $\Gamma(\boldsymbol{q})$ against ζ for scans taken at constant wavevector transfer $(\zeta, \zeta, 0)$ is shown in figure 6. The scans were taken at two different energy resolutions. The dotted lines in the figure show the caliper width of the resolution ellipsoid divided by 4. Scans for which the Lorentzian widths were narrower than this were not included in the analysis since the values for the widths could not be extracted reliably. The resolution corrections were made assuming a value for z of 0.8 and for κ of 0.01. It can be seen from figure 6 that on a log–log plot the Lorentzian widths lie on a good straight line up until $\zeta = 0.2$ when a slight curvature is observed towards a steeper gradient (and thus a larger value of the exponent). A power law fit to the first six points in figure 6 gives the exponent to be 0.79 ± 0.26. For $\zeta > 0.15$ this value increases presumably towards the value of 2 given by the RCO model, which we know from our results above T_C to give a good description of the spin dynamics away from the

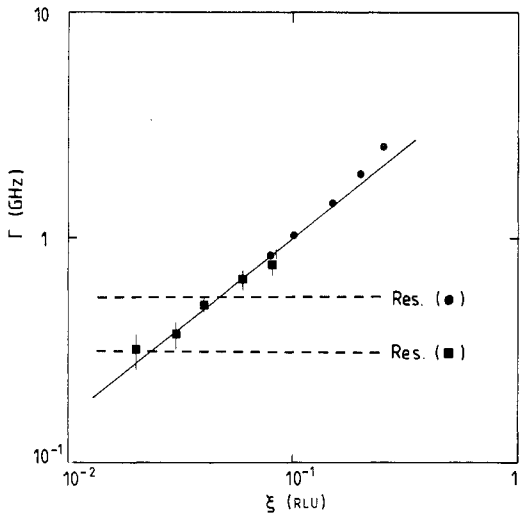

Figure 6. A log–log plot of the measured values of the characteristic frequencies for pure $LiTbF_4$ at $T = T_c = 2.89$ K, assuming a Lorentzian spectral weight function ($q = (\zeta, \zeta, 0)$). The broken lines mark the caliper resolution widths (HWHM) divided by 4.

critical region. κ was found to be small and was left equal to 0.01 RLU in the final fits. It could not be measured with great accuracy because the scans with $|q| \approx \kappa$ were resolution limited. We found the constant Γ_0 in equation (17) to be equal to 4.1 ± 0.1 GHz Å^2.

6.2.2. $LiTb_{0.6}Y_{0.4}F_4$. For the dilute system the data are harder to interpret since it seems clear that the inverse correlation range κ in the system was not small compared to the wavevector transfers used in the experiment. There are two possible reasons for this. First it may be that our temperature control was not sufficiently precise to enable us to get close enough to the transition ($T_C = 1.53$ K and our temperature precision was approximately ± 0.005 K), secondly it is possible that the quenched disorder in the sample somehow limits the spatial extent of the correlations. However it was difficult, in any case, to assign a unique correlation length because of the presence of extra intensity at small q in the data. This phenomenon was also observed by Kjaer *et al* (1989) in their neutron scattering study of $LiTb_{0.3}Y_{0.7}F_4$. A graph of χ_q as a function of q is shown in figure 7. The full line is a fit to the four points taken at the largest qs to the Lorentzian form, equation (15). From the graph one can clearly see extra intensity at small q. For the purposes of making resolution corrections a value of κ of 0.09 Å^{-1} was assumed in the final fits.

This anomalous scattering observed at small q also makes an interpretation of the observed linewidths difficult. A log–log plot of the characteristic frequencies is however shown in figure 8 from which one can see that the data do not lie on a unique straight line. This is not surprising however since as $|q| \to \kappa$ the linewidth becomes very dependent on the scaling function Ω in equation (17).

The data for $\zeta > 0.2$ (for which $|q| > \kappa$) however do seem to lie on a reasonable straight line in the log–log plot. A power law fit to these data gives an exponent of 0.8 ± 0.1, which we may tentatively identify with the dynamical critical exponent z, although it is not at all clear that this represents the asymptotic critical behaviour. Remarkably, perhaps, this is in good agreement with the value found for pure $LiTbF_4$ and it is a clear departure from the value of 2 expected if the RCO dynamics valid away from the critical region remain valid within the critical region. The constant Γ_0 is found

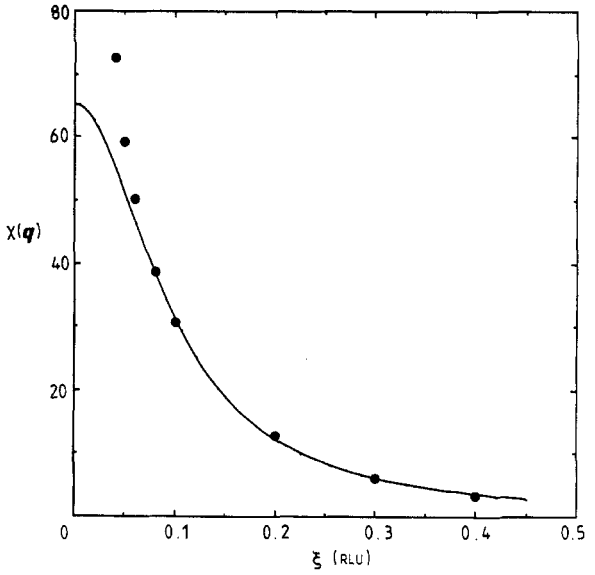

Figure 7. The wavevector-dependent susceptibility as defined in the text for $LiTb_{0.6}Y_{0.4}F_4$ as a function of q $(=(\zeta, 0, 0))$ at $T = T_c = 1.54$ K. The full circles are the data points and the full curve shows a Lorentzian fit to the four largest qs.

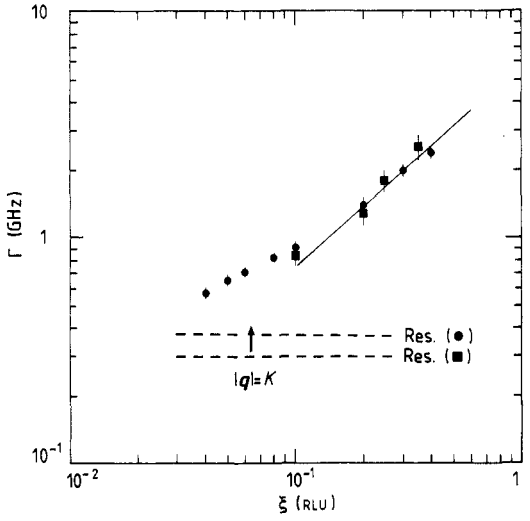

Figure 8. A log–log plot of the measured values of the characteristic frequencies for $LiTb_{0.6}Y_{0.4}F_4$ at $T = T_C = 1.54$ K $(q = (\zeta, 0, 0))$, assuming a Lorentzian spectral weight function. The broken lines mark the caliper resolution widths (HWHM) divided by 4.

in this case to be given by 4.7 ± 0.2 GHz Å^2. This is again in good agreement with the value for the pure system.

7. Summary and conclusions

We have measured the spin dynamics in $LiTbF_4$ and $LiTb_{0.6}Y_{0.4}F_4$ both above T_C in the paramagnetic region and at T_C. In both the pure and dilute materials, above T_C, we find the spin dynamics to be well described in a soft mode picture with the system displaying

a relaxation-coupled oscillation. The variation of the spectral response may be described fully by the dispersion and softening as $T \rightarrow T_C^+$ and $q \rightarrow 0$ of the magnetic excitons in the material. We find the damping of these excitons to be much greater in the pure system than the dilute system. The parameters we measure are in full agreement with those of Kötzler *et al* (1988) and are independent of wavevector and temperature.

At T_C we find this picture no longer gives a good description of the dynamics. As $q \rightarrow 0$ the data become less well fitted by the RCO lineshape. They are better fitted by a simple Lorentzian. In pure $LiTbF_4$ the characteristic (half area) frequency is found to be governed by a dynamical critical exponent $z = 0.79 \pm 0.26$.

In the dilute system an extra component is found to the scattering at small q which obscures the asymptotic behaviour. At larger q the characteristic frequency is found to be governed by an exponent $z = 0.8 \pm 0.1$, the same as that found in the pure system. A possible explanation for the low values of z is that what we observe in both systems is a cross-over to a regime in which the characteristic frequency is proportional to the exciton frequency itself which would give an exponent of 1.

The origin of the extra component to the scattering in the dilute system is unknown but presumably it must be associated with the presence of quenched disorder. We suggest tentatively the possibility that it be associated with the same clusters of spins responsible for the slow relaxation in the Griffiths phases of dilute magnets (see Lloyd and Mitchell 1989 and references therein) although our energy resolution is not good enough to see any manifestation of this in the dynamics. An interesting, although currently technically impossible, experiment would be a high resolution measurement of the energy spectrum of this extra intensity.

Acknowledgments

We wish to thank L D Cussen and C Carboni for experimental assistance and R Currat for helpful comments on the manuscript.

References

Aharony A 1976 *Phys. Rev.* B **13** 2092
Ahlers G, Korblitt A and Guggenheim H J 1975 *Phys. Rev. Lett.* **34** 1227
Als-Nielsen J 1976 *Phys. Rev. Lett.* **37** 1161
Als-Nielsen J, Holmes L M and Guggenheim H J 1974 *Phys. Rev. Lett.* **32** 610
Als-Nielsen J, Holmes L M, Krebs Larsen F and Guggenheim H J 1975 *Phys. Rev.* B **12** 191
De Gennes P G 1963 *Solid State Commun.* **1** 132
Dumont M 1984 *Physica* A **125** 124
Holmes L M, Als-Nielsen J and Guggenheim H J 1975 *Phys. Rev.* B **12** 180
Kjaer K, Als-Nielsen J, Laursen I and Krebs Larsen F 1989 *J. Phys.: Condens. Matter* **1** 5743
Kötzler J, Neuhaus-Steinmetz A, Froese A and Görlitz D 1988 *Phys. Rev. Lett.* **60** 647
Laursen I and Holmes L M 1974 *J. Phys. C: Solid State Phys.* **7** 3765
Lloyd R G and Mitchell P W 1989 *J. Phys.: Condens. Matter* **1** 5013
Lloyd R G, Mitchell P W, Ward R C C and Cherrill M 1988 *J. Physique Coll.* **49** C8 1047
Margarino J, Tuchendler J, Beauvillain P and Laursen I 1980 *Phys. Rev.* B **21** 18
Shirane G and Axe J D 1971 *Phys. Rev. Lett.* **27** 1803
Stephen M S and Aharony A 1981 *J. Phys. C: Solid State Phys.* **14** 1665
Stinchcombe R B 1973 *J. Phys. C: Solid State Phys.* **6** 2459
Wang Y and Cooper B R 1968 *Phys. Rev.* **172** 539
Young A P 1975 *J. Phys. C: Solid State Phys.* **8** L309
Youngblood R W, Aeppli G, Axe J D and Griffin J A 1982 *Phys. Rev. Lett.* **49** 1724